Article

Biophysical Analysis of the MHR Motif in Folding and Domain Swapping of the HIV Capsid Protein C-Terminal Domain

Rebeca Bocanegra,[1] Miguel Ángel Fuertes,[1] Alicia Rodríguez-Huete,[1] José Luis Neira,[2] and Mauricio G. Mateu[1,*]
[1]Centro de Biología Molecular Severo Ochoa (Consejo Superior de Investigaciones Científicas-Universidad Autónoma de Madrid), Madrid, Spain; and [2]Instituto de Biología Molecular y Celular, Universidad Miguel Hernández, Elche, and Instituto de Biocomputación y Física de los Sistemas Complejos, Zaragoza, Spain

ABSTRACT Infection by human immunodeficiency virus (HIV) depends on the function, in virion morphogenesis and other stages of the viral cycle, of a highly conserved structural element, the major homology region (MHR), within the carboxyterminal domain (CTD) of the capsid protein. In a modified CTD dimer, MHR is swapped between monomers. While no evidence for MHR swapping has been provided by structural models of retroviral capsids, it is unknown whether it may occur transiently along the virus assembly pathway. Whatever the case, the MHR-swapped dimer does provide a novel target for the development of anti-HIV drugs based on the concept of trapping a nonnative capsid protein conformation. We have carried out a thermodynamic and kinetic characterization of the domain-swapped CTD dimer in solution. The analysis includes a dissection of the role of conserved MHR residues and other amino acids at the dimerization interface in CTD folding, stability, and dimerization by domain swapping. The results revealed some energetic hotspots at the domain-swapped interface. In addition, many MHR residues that are not in the protein hydrophobic core were nevertheless found to be critical for folding and stability of the CTD monomer, which may dramatically slow down the swapping reaction. Conservation of MHR residues in retroviruses did not correlate with their contribution to domain swapping, but it did correlate with their importance for stable CTD folding. Because folding is required for capsid protein function, this remarkable MHR-mediated conformational stabilization of CTD may help to explain the functional roles of MHR not only during immature capsid assembly but in other processes associated with retrovirus infection. This energetic dissection of the dimerization interface in MHR-swapped CTD may also facilitate the design of anti-HIV compounds that inhibit capsid assembly by conformational trapping of swapped CTD dimers.

INTRODUCTION

During human immunodeficiency virus type 1 (HIV-1) morphogenesis (1–3), the viral Gag polyprotein (containing the capsid protein CA) assembles into a spherical capsid, which is enclosed in the immature virion. Gag is later cleaved, and free CA reassembles into a cone-shaped capsid within the mature, infectious virion.

The folded CA polypeptide is made of two domains (Fig. 1). The N-terminal domain (NTD) includes seven α-helices (helices 1–7) (4). The C-terminal domain (CTD) contains a 3_{10}-helix, an extended strand, and four α-helices (helices 8–11) (5) (Fig. 1 *a*).

Fitting the atomic structures of CA oligomers in cryo-electron microscopy, crystallography, or tomography density maps of authentic capsids or capsidlike particles yielded pseudoatomic models of immature (6–8) and mature (9–14) capsids. The models revealed several functionally relevant interfaces involving interactions between CA subunits (1–3,15,16). These findings are proving extremely helpful in the identification and characterization of capsid-assembly inhibitors that could lead to novel anti-HIV drugs (17–20).

A 20-residue structural element within the CTD, termed the major homology region (MHR) (5), exhibits a most conserved sequence, and this extreme conservation in an otherwise highly variable virus has long intrigued researchers. This motif is formed by an extended strand, a β-turn, and helix 8 (Fig. 1 *b*), and it contains conserved residues involved in a network of hydrogen bonds and hydrophobic contacts (5), which could stabilize the folded conformation (21). The MHR is critical to HIV-1 infection and, remarkably, has been found to be functionally involved in several different stages of the retroviral cycle, including immature capsid assembly (see, e.g., (22–29)).

In dimeric CA and CTD (both in solution and in most crystal forms) and in the mature HIV-1 capsid, the CTD monomers associate through the parallel packing of helix 9, which leads to a side-by-side dimer (5) (Fig. 1 *a*, *upper*). However, a structural homolog of retroviral CTD (a mammalian SCAN domain) forms a domain-swapped dimer in solution (30,31), and a mutant CTD (Δ177-CTD) from HIV-1, in which alanine 177 was deleted, was crystallized as a domain-swapped dimer by Ivanov et al. (32) (Fig. 1 *a*, *lower*). Interestingly, the exchanged part corresponds to the MHR motif, with several of its conserved residues being

Submitted May 9, 2014, and accepted for publication November 24, 2014.

*Correspondence: mgarcia@cbm.csic.es

Rebeca Bocanegra's present address is Centro Nacional de Biotecnología (Consejo Superior de Investigaciones Científicas), Campus de Cantoblanco, 28049 Madrid, Spain.

Editor: Ashok Deniz.

0006-3495/15/01/0338/12 $2.00

http://dx.doi.org/10.1016/j.bpj.2014.11.3472

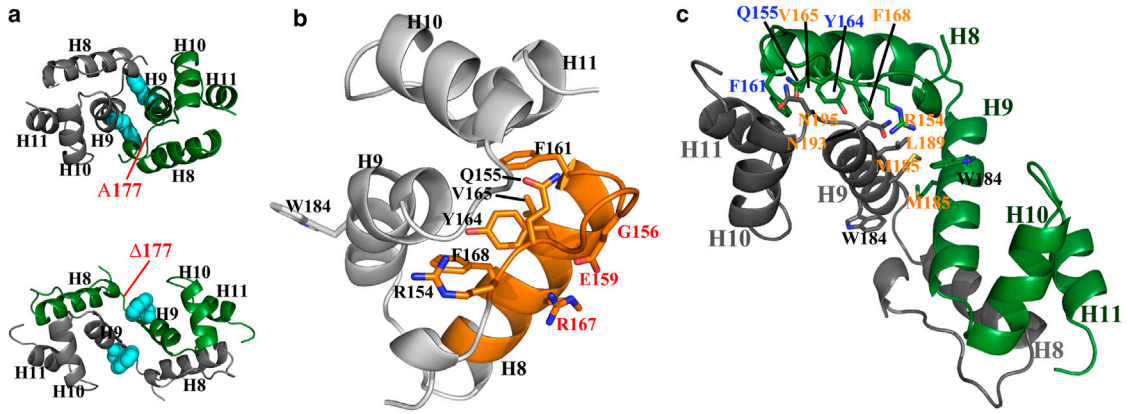

FIGURE 1 Molecular structures of CTD and Δ177-CTD. α-helices (H8–H11) are labeled. (*a*) Ribbon models of the crystal structures of the CTD side-by-side dimer (5) (Protein Data Bank (PDB) code 1A43) (*upper*) and the Δ177-CTD domain-swapped dimer (32) (PDB code 2ONT) (*lower*). W184 residues are represented as blue spacefilling models. The positions of A177 in CTD and its deletion in Δ177-CTD are indicated. (*b*) Ribbon model of a CTD monomer in the side-by-side dimer, with the MHR depicted in orange. Stick models are used to represent the side chains of W184, six conserved MHR residues that participate in domain swapping and were subjected to mutational analyses in this study (R154, Q155, Y164, V165, and F168 (*black labels*)), and three others (G156, E159, and R167 (*red labels*)) that do not participate in domain swapping and were subjected to mutation in a previous study (21). (*c*) Ribbon model of the structure of the Δ177-CTD domain-swapped dimer, in which interfacial MHR and non-MHR residues subjected to mutational analysis in this study are represented as stick models. Residues at the primary or secondary dimerization interfaces are labeled in blue and orange, respectively. Models were drawn using Pymol (71).

located at the swapped interface (Fig. 1 *c*). Because the MHR has a functional role in immature HIV-1 capsid assembly, Ivanov et al. suggested that MHR conservation could be due to its involvement in CTD dimerization by domain swapping during immature HIV assembly (32).

A recent, detailed pseudoatomic model (8) does not support the existence of the domain-swapped CTD conformation in the immature retroviral capsid. However, domain swapping, as well as other alternative modes of tertiary and quaternary organization detected in the conformationally dynamic CTD in oligomers or viral-like particles in vitro (e.g., (9,33–39)), could transiently occur along the still poorly known HIV-1 capsid assembly pathways (40–46).

Irrespective of whether CTD dimerization by domain swapping is a participant in HIV-1 morphogenesis (an unresolved question to date), it is a fact that under certain conditions (physiological or not), CTD can dimerize by swapping (32). Thus, a thorough biophysical characterization of this reaction could contribute to the development of an antiviral compound that could substantially stabilize (trap) this alternative CTD conformation. If the swapped dimer occurs on-pathway during HIV assembly, stabilizing the swapped intermediate could stop the reaction halfway. If the swapped dimer does not participate in virus assembly, converting CTD to this nonphysiological form would deplete the assembly reaction of the necessary capsid building blocks. Either way, HIV infection could be impaired. Experimental compounds capable of trapping CTD (within full-length CA or Gag) in other nonproductive conformations have already been identified (18,34,36).

Domain swapping has been observed in a significant and growing number of proteins ((47); for review, see Rousseau et al. (48,49)). In this process, two identical monomers exchange a part (called "domain") of their structure to form an intertwined dimer or other oligomer. The structure of the monomer is basically unchanged in the domain-swapped dimer, except in the linker that connects the exchanged part with the rest of the polypeptide. Thus, the exchanged part makes intermolecular interactions (the primary interface) in the domain-swapped dimer that essentially correspond to the intramolecular interactions it makes in the isolated monomer. Additional interactions between monomers in the domain-swapped dimer may occur (creating a secondary interface) (49). The biological significance of domain swapping is still uncertain in many cases, but in some proteins it may promote misfolding or regulate function (48,49) or stabilize viral particles (50). Studies on the thermodynamics and kinetics of a few domain-swapped cellular proteins provide important insights into this process and its biological roles (e.g., (48,49,51–59)).

In this study, we have carried out a thermodynamic and kinetic characterization of the domain-swapped Δ177-CTD dimer in solution with a twofold aim: 1) to provide biophysical evidence for or against domain swapping as a possible participant in HIV assembly and the main cause of MHR conservation and, eventually, to find alternative causes for such conservation; and 2) to characterize this alternative CTD dimerization, to provide further insights into protein domain swapping in general, and to facilitate the development of a novel HIV assembly inhibitor based on conformational trapping. The implications of the results for HIV biology and the design of anti-HIV drugs are discussed.

MATERIALS AND METHODS

Recombinant plasmids and site-directed mutagenesis

Plasmid pWISP98-85 containing the CA coding sequence from the pNL4.3 strain of HIV-1 was obtained through the AIDS Research and Reference Reagent Program, Division of AIDS, National Institute of Allergy and Infectious Diseases, National Institutes of Health (60). The triplet coding for A177 in CA was deleted using the Quik Change Site-Directed Mutagenesis kit (Stratagene, La Jolla, CA) to obtain plasmid pWISP98-85Δ177. The CTD-coding sequence with Ala177 deleted (Δ177-CTD) (32) in that plasmid was subcloned in plasmid pGEX-2T (GE Healthcare, Little Chalfont, United Kingdom) to obtain pGEX-2T-CTDΔ177. The construction of plasmid pET21-CTD containing the coding sequence for nonmutated CTD from strain BH10 of HIV-1 has been previously described (21). Deletion of the A177 codon in the CTD (BH10) and introduction of missense mutations in the CTD or in Δ177-CTD were performed on pET21-CTD or pGEX-2T-CTDΔ177 as appropriate using the procedures indicated above. The mutations were confirmed by sequencing the entire CTD coding region.

Protein expression and purification

CTD and mutants that do not carry the Δ177 deletion were purified as previously described (21). Δ177-CTD and mutants were expressed as fusion proteins with glutathione-S-transferase (GST) (32) and purified by affinity chromatography using GSTrap HP (GE Healthcare), following the instructions of the GST Gene Fusion System (GE Healthcare). GST was subsequently cleaved off by thrombin, and GST and thrombin were eliminated using GSTrap HP followed by HiTrap Benzamidine FF (GE Healthcare). Purified proteins were maintained in phosphate-buffered saline (PBS) with 5 mM dithiothreitol (DTT) at 4°C until dimerization equilibrium was reached. The protein solution was then applied to a size-exclusion chromatography (SEC) Superdex 75 column (GE Healthcare). Fractions containing monomer or dimer forms of Δ177-CTD were separately pooled, found free of contaminants as determined by sodium dodecyl sulfate-polyacrylamide gel electrophoresis, and stored at 4°C.

Fluorescence and circular dichroism spectroscopy

Fluorescence and circular dichroism (CD) analyses were done as previously described (21). The Trp fluorescence spectrum of Δ177-CTD monomer or dimer was obtained at 25°C; the effect of guanidinium hydrochloride (GdmHCl) was determined. The recorded far-UV CD spectra at 25°C were the averages of four scans between 190 and 250 nm obtained at a rate of 50 nm/min, a response time of 2 s, and a bandwidth of 1 nm.

Denaturation equilibrium analysis

Thermodynamic analysis of CTD unfolding was carried out by far-UV CD as described (21). The program KaleidaGraph (Synergy Software) was used for fitting all data obtained in thermodynamic and kinetic experiments. Chemical denaturation analysis of Δ177-CTD (pure monomer or dimer) was carried out by measuring the ellipticity at 222 nm of samples kept at 25°C and containing 20 μM protein (monomer concentration), unless otherwise specified, in 25 mM sodium phosphate buffer, pH 7.4, with different GdmHCl concentrations.

The data obtained in chemical denaturation equilibrium experiments were fitted to a unimolecular transition between native and denatured monomer as previously described (21). The thermodynamic parameters obtained were the concentration of denaturant at which 50% of the protein molecules are denatured ($[D]_{50\%}$), the variation in free energy with denaturant concentration (m), and the variation in free energy of the reaction extrapolated to absence of denaturant (ΔG_u^{H2O}).

Thermal denaturation analyses of Δ177-CTD, CTD, and mutants were carried out by monitoring the ellipticity at 222 nm of equivalent samples (without GdmHCl) subjected to a 4°C to 90°C thermal gradient (at a rate of 0.5°C/min). The data obtained in thermal denaturation equilibrium experiments were fitted to a unimolecular transition between native and denatured monomer by direct nonlinear fitting of the experimental ellipticity values, θ, in the equation (21)

$$\theta = [(\theta_{n0} + m_n T) + (\theta_{u0} + m_u T) \times \exp(-\Delta G_u/RT)]/[1 + \exp(-\Delta G_u/RT)], \quad (1)$$

where

$$\Delta G_u = \Delta H_u^{Tm}(1 - T/T_m) + \Delta C_p[T - T_m - T\ln(T/T_m)] \quad (2)$$

and θ is the experimental ellipticity obtained at a temperature T, R is the ideal gas constant, θ_{n0} and θ_{u0} are the ellipticity values, respectively, corresponding to the native (n) or denatured (u) states extrapolated to $T = 0$, m_n and m_u are the slopes of the baselines respectively preceding or following the transition region, T_m is the transition temperature, and ΔH_u^{Tm} is the variation in enthalpy of unfolding at the T_m. A ΔC_p value of 1200 cal/mol, in the normal range of heat capacity for protein denaturation processes (21), was assumed to fit the equation. As expected, changing this value to the lower or upper limit of the range determined for protein denaturation did not significantly change the T_m or ΔH_u^{Tm} values. Direct fitting yielded the values of θ_{n0}, θ_{u0}, m_n, m_u, T_m, and ΔH_u^{Tm}.

Dimerization equilibrium analysis

The Δ177-CTD monomer-dimer equilibrium was analyzed by SEC (55). Purified Δ177-CTD and mutants were maintained over the course of several weeks at high concentration (between 300 μM and 1 mM) until equilibrium was reached (as revealed by no significant further change in the dimer-to-monomer ratio). A volume of 100 μL of a protein solution at specified concentrations in PBS, pH 7.4, supplemented with 5 mM DTT was applied to a calibrated Superdex 75 analytical column (GE Healthcare) at 25°C, and the absorbance at 280 nm was monitored. The fractions of dimer and monomer were determined by measuring the areas of the peaks in the chromatogram and their concentrations were obtained at each total protein concentration tested. The equilibrium dissociation constant, K_d, was then directly calculated from the monomer (M) and dimer (D) concentrations (55):

$$K_d = [M]^2/[D]. \quad (3)$$

Kinetic analyses of Δ177-CTD dimerization and dissociation

The association and dissociation kinetics of Δ177-CTD were followed by analytical SEC at 25°C. To determine the association kinetics parameters, the monomeric form separated from the dimeric form by SEC was immediately concentrated to 300 μM, and 100 μL aliquots taken at different times after the dimer was isolated were applied to a Superdex 75 analytical column immediately after they were taken. The fractions of dimeric and monomeric forms were determined as described above. The fraction of dimer as a function of time was fitted to the equation that describes a second-order reaction from monomer to dimer:

$$D(t) = D_f - (A/(C_t\, k_{as} t + 1)), \quad (4)$$

where $D(t)$ is the fraction of dimer at time t, D_f is the fraction of dimer at infinite time, A is the amplitude (the difference between the initial and final values of D), and k_{as} is the association rate constant.

To determine the dissociation kinetics parameters, the dimeric species separated from the monomeric species by SEC was diluted to 20 μM, and 100 μL aliquots taken at different times after the dimer was isolated were applied to a Superdex 75 column. The fractions of dimer and monomer were then determined as indicated above. The fraction of dimer as a function of time could be fitted, as supported by residual analysis, to an equation that describes a sum of two first-order exponential decay reactions:

$$D(t) = D_f + A_1 \exp(-k_{dis1}t) + A_2 \exp(-k_{dis2}t), \quad (5)$$

where $D(t)$ is the fraction of dimer at time t, D_f is the fraction of dimer at infinite time, A_1 and A_2 are the amplitudes of the two processes considered, and k_{dis1} and k_{dis2} are the corresponding dissociation rate constants.

Kinetic analyses of canonical CTD dimerization and dissociation

The fast association and dissociation kinetics of the canonical CTD dimer were analyzed by following changes in intrinsic protein fluorescence at 25°C. A PiStar-180 stopped-flow fluorimeter (Applied Photophysics, Leatherhead, United Kingdom) set to an excitation wavelength of 295 nm was used to measure the variation in fluorescence at 320 nm of residue W184 in CTD.

To determine the association kinetics parameters, CTD (1 mM monomer) in sodium phosphate buffer, pH 7.4, was fully dissociated and denatured by addition to GdmHCl to 3 M or higher concentrations in different aliquots. For each aliquot, association of CTD monomers was initiated by 1:10 dilution in the same buffer without GdmHCl. At the final protein concentration (100 μM monomer) in the absence of GdmHCl, >90% of the protein is in dimeric form (61). The data obtained were fitted to the equation that describes a second-order reaction from monomer to dimer (62,63):

$$I(t) = I_f - (A/(C_t k_{as} t + 1)), \quad (6)$$

where $I(t)$ is the fluorescence intensity at time t, I_f is the fluorescence intensity at infinite time, A is the amplitude of the process, and k_{as} is the association rate constant.

To determine the dissociation kinetics parameters, aliquots of 100 μM CTD in sodium phosphate buffer, pH 7.4, were used. Dissociation of CTD dimers was initiated by a 1:10 dilution in 25 mM sodium phosphate buffer, pH 7.4, containing different concentrations of GdmHCl. At the final protein concentration (10 μM) most of the protein was in monomeric form. The data obtained were fitted to the equation that describes a first-order dissociation reaction from dimer to monomer:

$$I(t) = I_f + A \exp(-k_{dis}t), \quad (7)$$

where definitions of terms are the same as for Eq. 6, and $I(t)$ is the fluorescence intensity at time t, I_f is the fluorescence intensity at infinite time, A is the amplitude of the process and k_{dis} is the dissociation rate constant.

The natural logarithms of the different k_{as} and k_{dis} experimentally obtained using different denaturant concentrations were linearly fitted and extrapolated to obtain the k_{as} and k_{dis}, respectively, in the absence of denaturant.

NMR spectroscopy

One-dimensional ^{1}H-NMR data were acquired at 25°C using an Avance DRX-500 spectrometer (Bruker, Billerica, MA) equipped with a triple resonance probe and z-pulse field gradients. Processing of spectra was carried out with the TOPSPIN software. Spectra were acquired with a width of 12 ppm. Water was suppressed with the WATERGATE sequence (64).

RESULTS

Spectroscopic analysis of the Δ177-CTD monomer and dimer conformations

To biophysically characterize Δ177-CTD dimerization in solution, we constructed, expressed, and purified Δ177-CTD of the same viral strain (pNL4.3) used for crystallographic studies (32). The extremely slow interconversion between monomer and dimer forms allowed their separation by SEC and individual characterization.

The secondary structure of Δ177-CTD was probed by far-ultraviolet (far-UV) CD (Fig. 2 *a*). The spectra obtained for monomer and dimer revealed the helical content expected for folded CTD and were indistinguishable from each other (Fig. 2 *a*) and from those of the CTD monomer and dimer without the deletion (21). Thus, deletion of A177 has no effect on the secondary structure of the CTD monomer.

The tertiary environment of W184 in Δ177-CTD monomer and dimer was probed by measuring the intrinsic fluorescence. Fluorescence intensity was slightly reduced in the dimer relative to the monomer, but in both cases the emission maximum wavelength was ~350 nm (Fig. 2 *b*). Addition of GdmHCl up to 5 M did not increase the fluorescence intensity (results not shown). The maximum fluorescence emission wavelength in the nonmutated CTD monomer was also 350 nm, but was blueshifted to 338 nm in the nonmutated CTD dimer (21). These results are consistent with the different crystal structures of the side-by-side CTD dimer (5) and the domain-swapped Δ177-CTD dimer (32) (Fig. 1 *a*): in the former, W184 is buried in the dimerization interface, whereas in the latter, it is exposed to solvent (as in the isolated CTD monomer).

One-dimensional ^{1}H-NMR experiments (Fig.S1 in the Supporting Material) confirmed the exposure to solvent of W184 in the Δ177-CTD dimer in solution. The signal of the indole proton in the side-by-side CTD dimer was very broad and appeared at 10.65 ppm. In contrast, the same signal in the Δ177-CTD dimer was sharp and appeared at 10.35 ppm, close to the value expected in a random-coil polymer (10.20 ppm). In addition, comparison of NMR spectra revealed shifted peaks in the methyl region of the spectra of the Δ177-CTD dimer that may correspond to L188 and L189 methyls (the most up-fielded alkyl groups in the spectrum). This result indicates that the tertiary environment around those residues is also different in both dimers, again consistent with the crystal structures of the nonswapped and swapped forms of CTD.

Thermodynamic analysis of the Δ177-CTD monomer folding equilibrium

A previous study (21) showed that addition of GdmHCl to the CTD dimer leads to both dimer dissociation into folded monomers and monomer denaturation in a three-state reaction. However, dimer dissociation into folded monomers

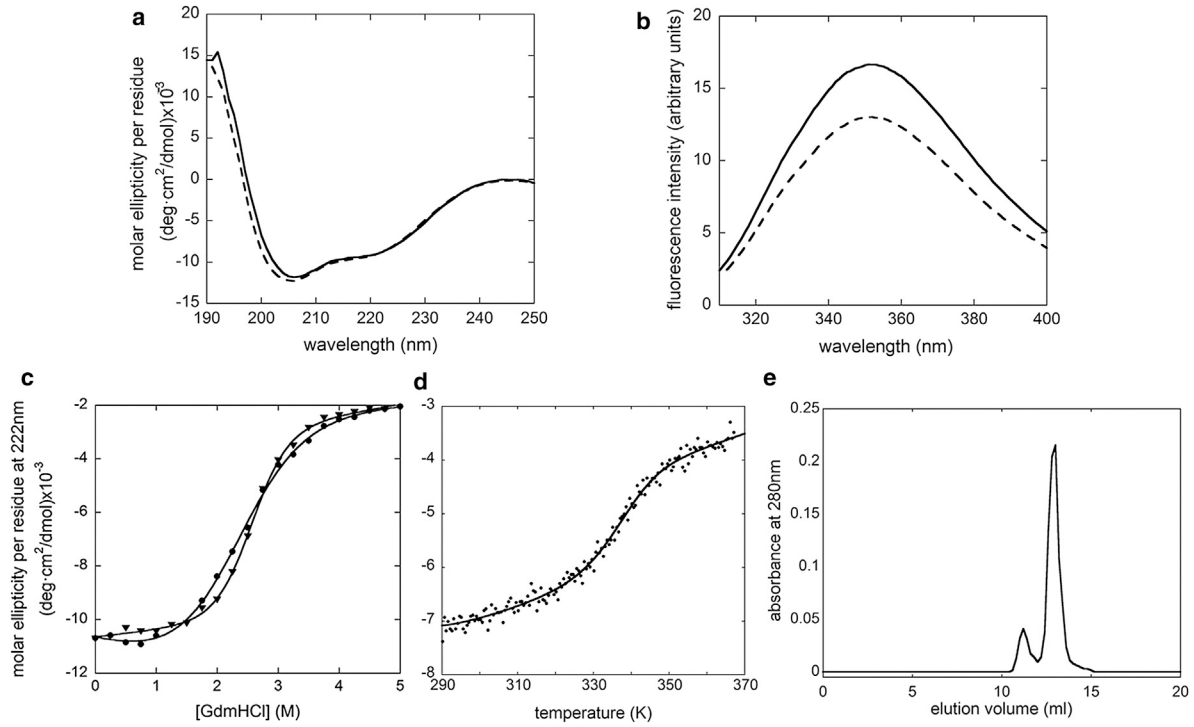

FIGURE 2 Spectroscopic and thermodynamic analyses of Δ177-CTD. (*a*) Far-UV CD spectra of the Δ177-CTD monomer (*solid line*) and dimer (*dashed line*). (*b*) Fluorescence spectra of Δ177-CTD monomer (*solid line*) and dimer (*dashed line*). (*c*) Chemical denaturation curve of the Δ177 monomer obtained by measuring the ellipticity at 222 nm as a function of GdmHCl concentration of Δ177-CTD monomer (*solid circles*) or dimer (*inverted triangles*). (*d*) Thermal denaturation curve of the Δ177-CTD monomer. Fitting of data in (*c*) and (*d*) is indicated by solid lines. The values obtained for the thermodynamic parameters are indicated in Table 1. In (*a*)–(*d*), 20 μM protein in 25 mM sodium phosphate pH 7.4 at 25°C were used. (*e*) Analytical SEC of Δ177-CTD at equilibrium between monomer and dimer, using 500 μM protein in PBS buffer, pH 7.4, and 5 mM DTT.

fully exposes the only Trp to solvent (leading to a change in Trp fluorescence), whereas it does not change the secondary structure of the protein (as observed by far-UV CD). In turn, denaturation of the folded monomers leads to no further exposure of Trp to solvent (no change in Trp fluorescence) but it does change the secondary structure of the protein (as measured by far-UV CD). Thus, dimer dissociation was spectroscopically silent when measuring the ellipticity signal at 222 nm by CD, whereas monomer unfolding was spectroscopically silent when measuring the Trp fluorescence signal on excitation at 295 nm. As a consequence, the two steps of the three-state (dissociation and unfolding) reaction can be thermodynamically (21) and kinetically analyzed separately as simple two-state reactions.

Like CTD, both monomer and dimer of Δ177-CTD showed the same far-UV CD spectrum, and Δ177-CTD dissociation was spectroscopically silent using CD. Thus, far-UV CD made it possible to specifically follow the folding/unfolding equilibrium of the Δ177-CTD monomer, irrespective of which form (monomer or dimer) was used, in chemical denaturation experiments as carried out for nonmutated CTD (21).

The unfolding equilibrium data obtained for Δ177-CTD in two representative experiments are shown in Fig. 2 *c*. They fitted well a two-state unimolecular transition (native monomer to denatured monomer). The process was fully reversible and, as expected, independent of protein concentration (Fig. S2). Again as expected, with either monomer or dimer, the values obtained for the thermodynamic parameters were not significantly different (Table 1). The values obtained for the Δ177-CTD monomer are also very similar to those obtained for nonmutated CTD under the same conditions (Table 1). The *m*-values obtained corresponded to those calculated (65) for the monomeric structures of Δ177-CTD and CTD (2.0 kcal mol^{-1} M^{-1} and 2.2 kcal mol^{-1} M^{-1}, respectively).

The unfolding equilibrium of the Δ177-CTD monomer was also analyzed in thermal denaturation experiments followed by far-UV-CD. The data obtained in a representative experiment are shown in Fig. 2 *d*. These data fitted very well a two-state unimolecular transition, and the process was reversible (Fig. S2). The values of the thermodynamic parameters obtained using Eqs. 1 and 2 were very similar to those obtained for nonmutated CTD under the same conditions (Table 1).

The above results revealed that Δ177-CTD and CTD monomers in solution have the same secondary structure, solvent exposure of W184, and thermodynamic stability. Thus, both monomers probably present quite similar structures in solution (except for a small region around Ala^{177}).

TABLE 1 Thermodynamic parameters of Δ177-CTD and CTD monomer unfolding, and kinetic and thermodynamic parameters for dimerization of Δ177-CTD and CTD

Protein	Thermodynamics of folding				
	ΔG_u^{H2O} (kcal mol^{-1})	m (kcal mol^{-1} M^{-1})	$[D]_{50\%}$(M)	T_m (°C)	ΔH_u^{Tm} (kcal mol^{-1})
Δ177-CTD	5.1 ± 0.2	1.95 ± 0.07	2.62 ± 0.01	62.7 ± 0.2	38 ± 2
CTD	4.4 ± 0.1	1.92 ± 0.04	2.29 ± 0.01	63.1 ± 0.1	45 ± 1
	Kinetics and thermodynamics of dimerization				
	k_{as} (M^{-1} s^{-1})	k_{dis} (s^{-1})	k_{dis}/k_{as} (μM)[a]	K_d (μM)[b]	
Δ177-CTD	(1.2 ± 0.2) × 10^{-2}	(7 ± 2) × 10^{-7} [c]	58 ± 9		
		(4.2 ± 0.5) × 10^{-5} [d]	3500 ± 185	2100 ± 1000	
CTD	(7.95 ± 0.02) × 10^{6}	100 ± 2	12.1 ± 0.1	8.3 ± 2.1	

Fitting values and errors are indicated.
[a]Equilibrium constant K_d calculated as the ratio between rate constants.
[b]Equilibrium constant K_d calculated in equilibrium experiments using SEC.
[c]Rate constant k_{dis1} corresponding to the slowest dissociation process.
[d]Rate constant k_{dis2} corresponding to the fastest dissociation process.

Thermodynamic analyses of Δ177-CTD dimerization equilibrium

Solutions of concentrated Δ177-CTD were left for several weeks until chemical equilibrium was reached and then subjected to analytical SEC. The chromatograms (Fig. 2 *e*) showed two peaks with apparent molecular masses of 13 kDa and 26 kDa. The somewhat increased apparent molecular masses relative to their true masses (9.5 kDa and 19 kDa) are likely due to the somewhat elongated shape of the CTD, which is more pronounced in the Δ177-CTD dimer. No additional oligomeric forms were significantly populated, even at very high protein concentration.

We analyzed the Δ177-CTD dimerization equilibrium at different pH values (from 5 to 9), ionic strengths (up to 1 M NaCl), and addition of DTT (to 5 mM) at different (0.3–1 mM) protein concentrations. At the highest protein concentrations, the maximum proportion of dimer at equilibrium was 20–25%. Starting with either monomer or dimer, the same monomer-dimer equilibrium was reestablished after close to one month at 25°C. After unfolding and refolding/reassociation of the monomer by heating to 95°C and cooling to 25°C, equilibrium was reached at a much faster rate (minutes) (Fig. S3).

The apparent dissociation equilibrium constant, K_d, was calculated from the proportion of monomer and dimer at different total protein concentrations (Eq. 3). In our standard conditions (PBS buffer, pH 7.4, 5 mM DTT, 25°C), the K_d value obtained was 2.1 ± 1.0 mM (Table 1). Δ177-CTD of a different HIV-1 strain (BH10), was also prepared and analyzed. Its K_d was ~5 mM (data not shown), on the same order as that of strain pNL4.3. By comparison, K_d of the side-by-side CTD dimer of the same strain under very similar conditions was 8 μM.

Kinetic analysis of Δ177-CTD dimerization and dissociation

To determine the association and dissociation rate constants of the Δ177-CTD dimer, we again took advantage of the extremely slow monomer-dimer interconversion. Both forms were separated by SEC and found to be essentially free of the other form. Isolated monomer (300 μM) and dimer (20 μM) were allowed to proceed toward equilibrium, and the dimer/monomer ratio at different times was estimated by SEC. This allowed a direct determination of the association and dissociation rate constants in the absence of any denaturing agent (Fig. 3, *a* and *b*).

The association kinetics showed a very good fit with Eq. 4, which describes a bimolecular reaction between two monomers to form a dimer (Fig. 3 *a*), which in turn yields the association rate constant (Table 1).

The dissociation kinetics could not be fitted to a single-exponential equation. However, the data could be very well fitted to an equation that describes two exponential unimolecular reactions (Eq. 5) with similar amplitudes and rate constants that differ by two orders of magnitude (Fig. 3 *b* and Table 1). The corresponding apparent dissociation equilibrium constants, calculated as the k_{dis}/k_{as} ratio, were K_{d1} = 3.5 mM and K_{d2} = 58 μM (Table 1). Thus, dissociation of domain-swapped Δ177-CTD may involve two different reactions. Though further investigation is required, a simple possibility is that the protein may be present in two similarly populated, conformationally nonidentical dimeric forms (indistinguishable by SEC); both dimeric forms could dissociate at different rates to yield the folded monomeric form. None of these forms correspond to the canonical dimer, as the dissociation rate constant of the latter was several orders of magnitude higher (see below). The form that dissociates relatively faster would be predominant, and its k_{dis}/k_{as} = 3.5 mM corresponds fairly well to the K_d =2.1 mM calculated from equilibrium experiments (Table 1). The slightly higher value of k_{dis}/k_{as} compared to K_d could be due to the fact that for the Δ177-CTD k_{as} calculation, we considered the association process only and assumed dissociation to be negligible. In fact, the values in Table 1 suggest a significant contribution of dissociation as the dimer is formed, and the k_{as} value obtained may be somewhat underestimated.

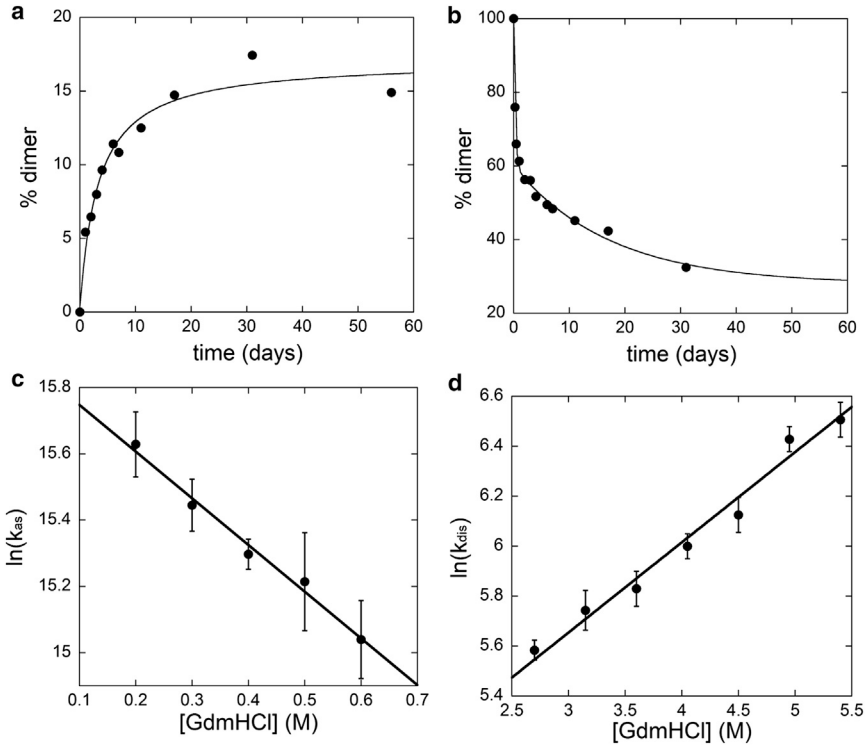

FIGURE 3 Kinetic analysis of association and dissociation of Δ177-CTD and CTD. (*a* and *b*) Δ177-CTD association (*a*) and dissociation kinetics (*b*). Errors are <10% of the measured value. (*c* and *d*) CTD association (*c*) and dissociation rate constants (*d*) as a function of denaturant concentration. Values correspond to the average of at least six kinetic traces. Fitting of data in (*a*)–(*d*) is indicated by solid lines. Error bars correspond to standard deviations. The values obtained for the kinetic parameters are indicated in Table 1.

Kinetic analysis of nonmutated CTD dimerization and dissociation

To compare the association and dissociation kinetics of Δ177-CTD with those of the side-by-side CTD dimer, we also had to determine the kinetic parameters of the latter, as they had not been obtained previously. CTD monomer unfolding was spectroscopically silent when Trp fluorescence was used as a probe (see above and Mateu (21)). Thus, only the dissociation and association rate constants influence the kinetics observed by following the Trp fluorescence intensity at 350 nm at different GdmHCl concentrations, and those constants could be directly determined in stopped-flow experiments (Fig. 3, *c* and *d*, and Table 1).

The association reaction was so fast that the initial part of the reaction was lost in the dead time of the instrument. However, as expected, the data obtained in repeated experiments fitted well an equation that describes a bimolecular reaction between two monomers to yield a dimer. Linear fitting of the $\ln(k_{as})$ values as a function of denaturant concentration (Fig. 3 *c*) and extrapolation to zero denaturant yielded k_{as}^{H2O} (Table 1). In this case, the values in Table 1 indicate that the contribution of k_{dis} is negligible. Thus, the rate constant value obtained should correspond to k_{as}.

The dissociation reaction was also very fast, and again, although the initial part of the reaction was lost in the dead time of the instrument, the data obtained in different experiments fitted well the expected single-exponential equation that describes a unimolecular dissociation reaction from dimer to monomers. Linear fitting of the $\ln(k_{dis})$ values as a function of denaturant concentration (Fig. 3 *d*) and extrapolation to zero denaturant yielded k_{dis}^{H2O} (Table 1). Because of the relatively high denaturant concentration and low protein concentration, the contribution of k_{as} to the experimental data under these conditions should be negligible, and the value obtained should correspond to k_{dis}.

The apparent dissociation equilibrium constant, K_d, calculated as the k_{dis}/k_{as} ratio, was 12.1 ± 0.1 μM (Table 1), very close to the K_d values obtained in equilibrium analyses under very similar conditions using analytical centrifugation (10 μM (5)) or SEC (8 μM (61)). Thus, loss of the initial part of the reactions in the dead time of the instrument did not have a significant effect on the estimation of the rate constants.

To sum up, under the conditions used, side-by-side dimerization of CTD is extremely fast, but the affinity constant is not high, because dimer dissociation is also very fast. In contrast, dimerization of Δ177-CTD is an extremely slow process, the rate of which can be greatly increased by previous thermal unfolding of the monomer. The affinity constant is very low, and it is not even lower because dissociation of the dimer is also very slow.

Mutational analysis of the role of conserved MHR residues and other interfacial residues in the thermodynamic stability of the CTD monomer

The above biophysical characterization allowed a molecular dissection of the relevance of MHR and other CTD residues

structurally involved in the domain-swapped interface (32) (Fig. 1 *c*), in terms of both folding and stability of the CTD monomer and dimerization affinity of Δ177-CTD. We chose for mutational analysis six MHR residues (Table 2).

Five of these residues are highly conserved in retroviruses and participate in hydrophobic contacts and/or hydrogen bonds between monomers in the domain-swapped dimer, whereas R154 is less conserved and participates in a few interactions only (Table 2). The side chains of three of these residues (Q155, F161, and Y164) belong to the primary interface (sensu stricto), whereas those of three others (R154, V165, and F168) belong to the secondary interface in the domain-swapped dimer (Fig. 1 *c* and Table 2). Only one other MHR residue (Y169) participates in intermonomer interactions in the swapped dimer, but this residue was not chosen for mutation, as it is less conserved. In addition, we chose four non-MHR residues (M185, L189, N193, and N195) involved in the highest numbers of hydrophobic contacts and/or hydrogen bonds between monomers in the swapped dimer (Table 2). These four residues belong to the secondary interface (Fig. 1 *c* and Table 2).

The parental fusion protein GST-Δ177-CTD and 7 of the 10 mutants could be expressed, and after cleavage, the isolated domain could be obtained in soluble form. However, these mutations led to levels of soluble CTD that were reduced to different extents, and mutations of MHR residues F168 and N193 greatly favored aggregation. In addition, mutation of any of the three MHR residues at the primary interface led to proteolytic degradation of Δ177-CTD during expression of the fusion protein, usually yielding GST only. In some preparations of these three mutants, a very small amount of GST-Δ177-CTD could be obtained initially, but after thrombin digestion, only GST remained (i.e., without Δ177-CTD). These observations indicate that these three CTD mutants are unable to fold under those conditions.

All seven Δ177-CTD mutants that could be obtained in a soluble, folded state showed the same minima at 208 and 220 nm as the parent protein Δ177-CTD by far-UV CD. They also showed the same maximum around 350 nm in their fluorescence emission spectrum, although in two of them (L189A and V165A) minor blue shifts were observed that could be due to small differences in the tertiary environment of W184. All CD and fluorescence spectra were superimposable on those of the parental Δ177-CTD except for the three mutants with the highest tendencies to aggregate, in which the ellipticity and fluorescence intensity were proportionally reduced at all wavelengths, most likely due to partial aggregation during the analyses (results not shown). The thermodynamic stability of the seven Δ177-CTD mutants that were capable of folding was then determined in thermal denaturation experiments like that shown in Fig. 2 *d* (Table 2). Mutation of most residues led to a substantial destabilization of the folded CTD monomer.

Most MHR residues with a high degree of conservation among retroviruses (66) were found to be important for CTD folding/stability. These residues include the three residues that had been previously analyzed (21), E159, R167, and G156, as well as Q155, F161, Y164, V165, and F168 (Table 2). In contrast, MHR residue R154, which is much less conserved than the others, barely contributed to CTD stability (Table 2).

It could be argued that the observed disruptive or destabilizing effects of the analyzed mutations on the folding and stability of the Δ177-CTD monomer could be influenced

TABLE 2 Mutational analysis of the role of interfacial residues in thermodynamic stability of the Δ177-CTD and CTD monomers and in the affinity of Δ177-CTD dimerization

Mutation	Location in CTD and in swapped interface[a]		% C[b]	Interactions[c]		Δ177-CTD			CTD	
				Δ177-CTD	CTD	T_m (°C)	ΔH_u^{Tm} (kcal mol^{-1})	K_d (mM)	T_m (°C)	ΔH_u^{Tm} (kcal mol^{-1})
Parent						62.7 ± 0.2	38 ± 2	2.1	63.1 ± 0.1	45 ± 1
Q155A	MHR	Prim	100	1/26/7	1/46/18	unfolded			unfolded	
F161A	MHR	Prim	71	0/34/25	0/40/32	unfolded			unfolded	
Y164A	MHR	Prim	100	1/33/16	1/38/19	unfolded			unfolded	
R154A	MHR	Sec	50	0/5/1	0/3/2	59.2 ± 0.1	49 ± 3	1.1	62.1 ± 0.6	44 ± 3
V165A	MHR	Sec	93	0/12/9	0/5/5	59.6 ± 0.1	50 ± 3	1.2	47.9 ± 1.0	27 ± 2
F168A	MHR	Sec	100	0/30/26	0/33/27	47.0 ± 2.0	31 ± 7	10.9	58.8 ± 0.6	37 ± 1
M185A	h9	Sec	21	0/20/12	0/6/4	67.1 ± 0.1	61 ± 4	2.3	56.0 ± 1.0	27 ± 8
L189A	h9	Sec	50	0/7/7	0/4/3	61.1 ± 0.1	51 ± 3	2.2	ND	ND
N193A	h9	Sec	50	1/9/1	1/8/1	52.2 ± 0.8	51 ± 9	ND[d]	52.0 ± 5.0	17 ± 8
N195A	L9-10	Sec	50	1/17/4	1/8/1	56.0 ± 0.2	44 ± 7	6.9	ND	ND

Fitting values and errors are indicated. For K_d values, no fitting errors are applicable as these values were directly determined by measuring the areas corresponding to monomer and dimer SEC peaks at equilibrium. The errors between repeated experiments were <2°C for T_m, <10 kcal mol^{-1} for ΔH_u^{Tm}, and <1 mM for K_d. h9, helix 9; L9-10, loop between helices 9 and 10; Prim, primary interface; Sec, secondary interface; ND, not determined.

[a]Location of the original residue.

[b]Percent conservation of the original residue in retroviruses (66).

[c]Interactions of the original residue, expressed as number of hydrogen bonds/total van der Waals contacts/carbon-carbon contacts, determined using the program WHATIF (70) and a cutoff distance of 3.5 Å (for H-bonds) and 1 Å longer than the sum of van der Waals ratios (for vdW contacts).

[d]For N193A, the K_d could not be determined due to the small amounts of soluble protein obtained and its tendency to aggregate during the long incubation time (weeks) required for equilibrium analysis using SEC.

by deletion of A177. Thus, we introduced individual alanine mutations of the same six MHR residues, as well as of two of the four nonMHR residues, in the intact CTD of the same HIV-1 strain; we then tested for their effects on CTD monomer folding and stability, as described above for Δ177-CTD (Table 2). In general, the results were qualitatively similar to those obtained for Δ177-CTD: In both cases, mutants Q155A, F161A, and Y164A led to unfolded protein; N193A and R154A had a large or small effect, respectively, on protein stability. V165A, F168A, and M185A, however, led to quantitatively different destabilizing effects that suggest some local differences in the tertiary structure of the monomer due to the A177 deletion in Δ177-CTD.

Mutational analysis of the role of conserved MHR residues and other interfacial residues in the affinity of Δ177-CTD dimerization

The effect of mutation of the three conserved MHR residues at the primary interface on Δ177-CTD dimerization could not be tested, because these mutations completely prevented stable folding of the CTD monomer (see previous section). However, six Δ177-CTD mutants could be obtained in folded, soluble form and their aggregation could be prevented even at the high concentration needed for analysis of the Δ177-CTD dimerization equilibrium. These mutations involved two highly conserved MHR residues (V165 and F168), a less conserved MHR residue (R154), and three non-MHR residues (M185, L189, and N195), all at the secondary interface in the domain-swapped dimer (Fig. 1 *c* and Table 2). The dimerization affinity of these mutants was determined by SEC (Table 2).

Of the six mutations tested, only F168A and N195A led to a significant increase in the apparent dissociation equilibrium constant, K_d. Thus, only one of the three highly conserved MHR residues tested (F168) significantly contributes to Δ177-CTD dimerization. The two other MHR residues tested (R154A and V165A) are not involved in dimerization energetics.

In summary, for MHR residues, no correspondence was found between their conservation in retroviruses and their contribution to the affinity of Δ177-CTD dimerization. In contrast, nearly all highly conserved MHR residues are involved in the stable folding of the CTD monomer, whereas the less conserved MHR residue, R154, makes no significant contribution.

DISCUSSION

Thermodynamic and kinetics of domain swapping in CTD: comparison with other proteins and dissection of a domain-swapped interface

Δ177-CTD crystallizes only as a domain-swapped dimer, but it could be argued that the dimer it forms in solution is not domain-swapped. A considerable body of evidence, discussed in this section, clearly indicates that the Δ177-CTD dimer in solution is not the canonical CTD dimer but a domain-swapped dimer. The evidence is largely based on what has been learned about domain swapping in general from studies carried out with a number of domain-swapped dimers (48,49). Despite the wide differences among them in structure, function, and evolutionary origin, they present common features that are exclusive of their dimerization by domain swapping. These include extremely low association and dissociation rate constants and a dramatic acceleration of dimerization by heating and cooling (48,49). Such features are explained because domain swapping usually requires substantial unfolding of the monomer before the domain can be swapped (55,58). Dimerization reactions that do not involve swapping show no such behavior, because they do not require substantial monomer unfolding.

With the above specific features of domain swapping in mind, the following evidence clearly supports that the Δ177-CTD dimer in solution is domain-swapped. 1) Association and dissociation rate constants are an extremely low hallmark of domain-swapped dimers. 2) Dimerization is extremely accelerated (from weeks to minutes) by heating and cooling, another telling signature of domain swapping, as discussed above. 3) In the Δ177-CTD dimer, both in solution and in crystal form, residues F168 and N195 are involved in dimerization. 4) In the Δ177-CTD dimer, both in solution and in crystal form, W184 is fully exposed to solvent, as indicated by both fluorescence and NMR. 5) NMR results also suggest that the environment around the L188 and L189 side chains is altered in the Δ177-CTD dimer in solution, as would be expected if it is swapped. 6) The Δ177-CTD dimer, both in solution and in crystal form, has a shape that is more elongated than that of the canonical CTD dimer. All these results taken together provide strong evidence that Δ177-CTD forms a noncanonical, domain-swapped dimer in solution, in agreement with its structure as determined by x-ray crystallography.

The K_d for the domain-swapped SCAN dimer (the only known homolog of retroviral CTD) has not been determined, but no traces of monomer were observed by SEC at 225 μM (30), which suggests a K_d of <10 μM. Unlike SCAN, and even with A177 deleted, the K_d obtained for Δ177-CTD was as high as 2.1 mM. A similar value was obtained for the domain-swapped p13suc1 dimer (K_d $=1.8$ mM), but this value was for the natural domain; some deletions in the p13suc1 hinge led to a much lower K_d (55). Thus, although the CTD of HIV-1 CA can dimerize through domain swapping, its propensity to do so is marginal compared to other domain-swapping proteins.

As for other domain-swapped dimers, the extremely slow association and dissociation rates of Δ177-CTD and the dramatic reduction in time required to reach equilibrium indicates the existence of a large kinetic barrier for dimerization. In the CTD monomer, many conserved

residues in the region to be swapped have numerous interactions with the rest of the polypeptide, and our thermodynamic analysis showed that these residues are critically involved in stabilizing the monomer. Domain swapping requires disruption of all these energetically important interactions. These observations suggest that the transition state for interconversion between Δ177-CTD monomer and swapped dimer may be a substantially unfolded form of the protein.

Mutational analyses allowed the identification of a few CTD residues at the swapped interface that are energetically important for folding and stability and/or dimerization by swapping. Three residues (Q155, F161, and Y164) involved in multiple intersubunit interactions at the primary interface were critical for CTD monomer folding and stability. Of the six tested residues at the secondary interface in Δ177-CTD, only the two that are involved in a substantial number of interactions in both monomer and swapped dimer (F168 and N195) significantly favor the domain-swapped dimer relative to the free monomer.

To sum up, the Δ177-CTD domain-swapped interface includes several residues that are required for folding and stability of the monomer. The strong interactions these residues establish in the monomer may dramatically slow down dimerization by domain swapping. A few residues at the swapped interface define a limited number of energetic hotspots of Δ177-CTD dimerization.

Is CTD dimerization by domain swapping involved in HIV-1 capsid assembly, and could it provide a novel target for antiviral intervention?

Although MHR swapping does not appear to be present in assembled retrovirus capsids (8,13,14), it has been suggested that it could still transiently occur, either on- or off-pathway, during the assembly reaction. This possibility may be pondered in the light of the results presented here on the thermodynamics and kinetics of Δ177-CTD dimerization by domain swapping in solution.

First, even after engineering a deletion that greatly favors swapping, the K_d is >2 mM. This corresponds to a marginal intrinsic propensity compared to those observed for the homologous SCAN domain and other domain-swapping proteins. A most serious difficulty for domain swapping in CTD is that several residues in the motif to be swapped (the MHR) are heavily involved in energetically important intramonomer interactions that must be disrupted before the swapped dimer can be formed. This leads to a very high kinetic barrier and to extremely slow association and dissociation. It has been suggested that the process could be speeded up in vivo by coupling with some other binding event, such as association of the nucleocapsid domain in Gag with the viral RNA (67), and macromolecular crowding effects could also help (68,69). However, the observed k_{as} would need to increase by as many as five or more orders of magnitude to complete the process in seconds or minutes.

A strong argument for a transient role of MHR swapping during HIV-1 assembly could still be made if there were a correspondence between evolutionary conservation of MHR residues in retroviruses and net energetic contribution to Δ177-CTD dimerization by domain swapping (32,67). However, no such correspondence was found in our mutational analysis of MHR residues.

In summary, the above observations do not provide support for even transient MHR swapping during HIV capsid assembly. In fact, the quite marginal propensity of the conformationally plastic CTD to dimerize by domain swapping could be an evolutionary remnant of a reaction that at present may be biologically relevant only in some homologous protein (e.g., the mammalian SCAN domain). However, it cannot be excluded that a combination of structural context, nucleation, coupled reactions, and macromolecular crowding effects could lead to transient MHR swapping during HIV capsid assembly in the cell.

In our opinion, even though MHR swapping may not occur during HIV morphogenesis, it definitely offers a novel approach for anti-HIV intervention. The exclusive presence of a secondary interface in the domain-swapped dimer, and our energetic dissection of the swapped interface, may facilitate the design of compounds capable of specific binding to the swapped dimer. Such compounds could promote MHR-swapping in Gag and/or free CA by stabilizing the secondary interface, thus inhibiting HIV capsid assembly and viral infection by conformational trapping.

A critical role of conserved MHR residues in folding and stability of the CTD monomer may help to explain the multiple biological effects of the MHR in retrovirus infection

The nonswapped MHR motif may participate in CTD-CTD recognition in the immature retroviral capsid (8), which provides a simple structural basis for the detrimental effects in immature capsid assembly caused by mutations in the MHR. Still, one might wonder why the MHR is so conspicuously conserved relative to other structural elements that are critically involved in intersubunit recognition in the immature (or mature) capsid. Moreover, the MHR also has been found to be functionally involved in other steps of the viral cycle.

In this study, we found that all eight highly conserved MHR residues tested (five in this study and three others during an early thermodynamic analysis of the side-by-side CTD dimer (21)) are required for folding and stability of the CTD monomer. Also, we detected a correlation between their conservation and their importance for folding and stability. These effects were rather unexpected. First, they were observed for nearly half of the residues in a single small (20-amino-acid) structural element within a protein domain.

Second, most of those eight conserved MHR residues are not in the protein hydrophobic core; in fact, they have polar, solvent-exposed side chains. As expected, alanine mutation of several other polar and apolar residues in CTD, including those at the side-by-side dimerization interface and some other buried residues, generally had no such dramatic effects on monomer folding whatsoever (61). To our knowledge, this is a rather unique situation in proteins. The MHR appears to constitute a self-structured subdomain with a critical role in folding and stability of the CTD of the retroviral capsid protein.

Based on the above observations we propose that in addition to the detected direct functional roles of the MHR in retroviruses, the unusually important role of many MHR residues in CTD folding helps to explain their high conservation and biological importance. Mutations in the MHR impair CTD folding and facilitate degradation or aggregation, reducing the availability of correctly folded Gag and CA, not only for immature capsid assembly but also in other stages of the retroviral cycle in which these proteins are involved.

SUPPORTING MATERIAL

Three figures are available at http://www.biophysj.org/biophysj/supplemental/S0006-3495(14)04685-2.

ACKNOWLEDGMENTS

We thank Francisco N. Barrera for help with the stopped-flow experiments. Plasmid pWISP98-85 was obtained through the AIDS Research and Reference Reagent Program, Division of AIDS, National Institute of Allergy and Infectious Diseases, National Institutes of Health. M.G.M. is an associate member of the Institute of Biocomputation and Physics of Complex Systems, Zaragoza, Spain.

Work in M.G.M.'s laboratory is funded by grants from the Spanish Government (BIO2012-37649) and Comunidad de Madrid (S-2009/MAT/1467) and by an institutional grant from Fundación Ramón Areces. Work in J.L.N.'s laboratory is funded by grants from the Spanish Government (CTQ2011-24393 and CSD2008-00005) and Generalitat Valenciana (Prometeo 2013/18).

REFERENCES

1. Briggs, J. A., and H.-G. Kräusslich. 2011. The molecular architecture of HIV. *J. Mol. Biol.* 410:491–500.
2. Ganser-Pornillos, B. K., M. Yeager, and O. Pornillos. 2012. Assembly and architecture of HIV. *Adv. Exp. Med. Biol.* 726:441–465.
3. Sundquist, W. I., and H.-G. Kräusslich. 2012. HIV-1 assembly, budding, and maturation. *Cold Spring Harb. Perspect. Med.* 2:a006924.
4. Gitti, R. K., B. M. Lee, …, W. I. Sundquist. 1996. Structure of the amino-terminal core domain of the HIV-1 capsid protein. *Science.* 273:231–235.
5. Gamble, T. R., S. Yoo, …, C. P. Hill. 1997. Structure of the carboxyl-terminal dimerization domain of the HIV-1 capsid protein. *Science.* 278:849–853.
6. Wright, E. R., J. B. Schooler, …, G. J. Jensen. 2007. Electron cryotomography of immature HIV-1 virions reveals the structure of the CA and SP1 Gag shells. *EMBO J.* 26:2218–2226.
7. Briggs, J. A. G., J. D. Riches, …, H. G. Kräusslich. 2009. Structure and assembly of immature HIV. *Proc. Natl. Acad. Sci. USA.* 106:11090–11095.
8. Bharat, T. A., N. E. Davey, …, J. A. Briggs. 2012. Structure of the immature retroviral capsid at 8 Å resolution by cryo-electron microscopy. *Nature.* 487:385–389.
9. Ganser-Pornillos, B. K., A. Cheng, and M. Yeager. 2007. Structure of full-length HIV-1 CA: a model for the mature capsid lattice. *Cell.* 131:70–79.
10. Pornillos, O., B. K. Ganser-Pornillos, …, M. Yeager. 2009. X-ray structures of the hexameric building block of the HIV capsid. *Cell.* 137:1282–1292.
11. Byeon, I.-J. L., X. Meng, …, A. M. Gronenborn. 2009. Structural convergence between cryo-EM and NMR reveals intersubunit interactions critical for HIV-1 capsid function. *Cell.* 139:780–790.
12. Cardone, G., J. G. Purdy, …, A. C. Steven. 2009. Visualization of a missing link in retrovirus capsid assembly. *Nature.* 457:694–698.
13. Pornillos, O., B. K. Ganser-Pornillos, and M. Yeager. 2011. Atomic-level modelling of the HIV capsid. *Nature.* 469:424–427.
14. Zhao, G., J. R. Perilla, …, P. Zhang. 2013. Mature HIV-1 capsid structure by cryo-electron microscopy and all-atom molecular dynamics. *Nature.* 497:643–646.
15. Ganser-Pornillos, B. K., M. Yeager, and W. I. Sundquist. 2008. The structural biology of HIV assembly. *Curr. Opin. Struct. Biol.* 18: 203–217.
16. Mateu, M. G. 2009. The capsid protein of human immunodeficiency virus: intersubunit interactions during virus assembly. *FEBS J.* 276:6098–6109.
17. Prevelige, Jr., P. E. 2011. New approaches for antiviral targeting of HIV assembly. *J. Mol. Biol.* 410:634–640.
18. Bocanegra, R., A. Rodríguez-Huete, …, M. G. Mateu. 2012. Molecular recognition in the human immunodeficiency virus capsid and antiviral design. *Virus Res.* 169:388–410.
19. Waheed, A. A., and E. O. Freed. 2012. HIV type 1 Gag as a target for antiviral therapy. *AIDS Res. Hum. Retroviruses.* 28:54–75.
20. Domenech, R., and J. L. Neira. 2013. The HIV-1 capsid protein as a drug target: recent advances and future prospects. *Curr. Protein Pept. Sci.* 14:658–668.
21. Mateu, M. G. 2002. Conformational stability of dimeric and monomeric forms of the C-terminal domain of human immunodeficiency virus-1 capsid protein. *J. Mol. Biol.* 318:519–531.
22. Strambio-de-Castillia, C., and E. Hunter. 1992. Mutational analysis of the major homology region of Mason-Pfizer monkey virus by use of saturation mutagenesis. *J. Virol.* 66:7021–7032.
23. Mammano, F., A. Ohagen, …, H. G. Göttlinger. 1994. Role of the major homology region of human immunodeficiency virus type 1 in virion morphogenesis. *J. Virol.* 68:4927–4936.
24. Craven, R. C., A. E. Leure-duPree, …, J. W. Wills. 1995. Genetic analysis of the major homology region of the Rous sarcoma virus Gag protein. *J. Virol.* 69:4213–4227.
25. Orlinsky, K. J., J. Gu, …, T. M. Menees. 1996. Mutations in the Ty3 major homology region affect multiple steps in Ty3 retrotransposition. *J. Virol.* 70:3440–3448.
26. Provitera, P., A. Goff, …, S. Scarlata. 2001. Role of the major homology region in assembly of HIV-1 Gag. *Biochemistry.* 40:5565–5572.
27. von Schwedler, U. K., K. M. Stray, …, W. I. Sundquist. 2003. Functional surfaces of the human immunodeficiency virus type 1 capsid protein. *J. Virol.* 77:5439–5450.
28. Chang, Y. F., S. M. Wang, …, C. T. Wang. 2007. Mutations in capsid major homology region affect assembly and membrane affinity of HIV-1 Gag. *J. Mol. Biol.* 370:585–597.

29. Purdy, J. G., J. M. Flanagan, …, R. C. Craven. 2008. Critical role of conserved hydrophobic residues within the major homology region in mature retroviral capsid assembly. *J. Virol.* 82:5951–5961.

30. Stone, J. R., J. L. Maki, …, T. Collins. 2002. The SCAN domain of ZNF174 is a dimer. *J. Biol. Chem.* 277:5448–5452.

31. Ivanov, D., J. R. Stone, …, G. Wagner. 2005. Mammalian SCAN domain dimer is a domain-swapped homolog of the HIV capsid C-terminal domain. *Mol. Cell.* 17:137–143.

32. Ivanov, D., O. V. Tsodikov, …, T. Collins. 2007. Domain-swapped dimerization of the HIV-1 capsid C-terminal domain. *Proc. Natl. Acad. Sci. USA.* 104:4353–4358.

33. Alcaraz, L. A., M. del Alamo, …, J. L. Neira. 2007. Flexibility in HIV-1 assembly subunits: solution structure of the monomeric C-terminal domain of the capsid protein. *Biophys. J.* 93:1264–1276.

34. Bartonova, V., S. Igonet, …, H.-G. Kraüsslich. 2008. Residues in the HIV-1 capsid assembly inhibitor binding site are essential for maintaining the assembly-competent quaternary structure of the capsid protein. *J. Biol. Chem.* 283:32024–32033.

35. Wong, H. C., R. Shin, and N. R. Krishna. 2008. Solution structure of a double mutant of the carboxy-terminal dimerization domain of the HIV-1 capsid protein. *Biochemistry.* 47:2289–2297.

36. Du, S., L. Betts, …, J. I. Yeh. 2011. Structure of the HIV-1 full-length capsid protein in a conformationally trapped unassembled state induced by small-molecule binding. *J. Mol. Biol.* 406:371–386.

37. Byeon, I. J., G. Hou, …, T. Polenova. 2012. Motions on the millisecond time scale and multiple conformations of HIV-1 capsid protein: implications for structural polymorphism of CA assemblies. *J. Am. Chem. Soc.* 134:6455–6466.

38. Lampel, A., O. Yaniv, …, F. Frolow. 2013. A triclinic crystal structure of the carboxy-terminal domain of HIV-1 capsid protein with four molecules in the asymmetric unit reveals a novel packing interface. *Acta Crystallogr. Sect. F Struct. Biol. Cryst. Commun.* 69:602–606.

39. Bayro, M. J., B. Chen, …, R. Tycko. 2014. Site-specific structural variations accompanying tubular assembly of the HIV-1 capsid protein. *J. Mol. Biol.* 426:1109–1127.

40. Ehrlich, L. S., T. Liu, …, C. A. Carter. 2001. HIV-1 capsid protein forms spherical (immature-like) and tubular (mature-like) particles in vitro: structure switching by pH-induced conformational changes. *Biophys. J.* 81:586–594.

41. Morikawa, Y., T. Goto, and F. Momose. 2004. Human immunodeficiency virus type 1 Gag assembly through assembly intermediates. *J. Biol. Chem.* 279:31964–31972.

42. Lingappa, J. R., and B. K. Thielen. 2009. Assembly of immature HIV-1 capsids using a cell-free system. *Methods Mol. Biol.* 485:185–195.

43. López, C. S., J. D. Eccles, …, E. Barklis. 2011. Determinants of the HIV-1 core assembly pathway. *Virology.* 417:137–146.

44. Chen, B., and R. Tycko. 2011. Simulated self-assembly of the HIV-1 capsid: protein shape and native contacts are sufficient for two-dimensional lattice formation. *Biophys. J.* 100:3035–3044.

45. Tsiang, M., A. Niedziela-Majka, …, R. Sakowicz. 2012. A trimer of dimers is the basic building block for human immunodeficiency virus-1 capsid assembly. *Biochemistry.* 51:4416–4428.

46. Bocanegra, R., C. Alfonso, …, M. G. Mateu. 2013. Association equilibrium of the HIV-1 capsid protein in a crowded medium reveals that hexamerization during capsid assembly requires a functional C-domain dimerization interface. *Biophys. J.* 104:884–893.

47. Bennett, M. J., S. Choe, and D. Eisenberg. 1994. Domain swapping: entangling alliances between proteins. *Proc. Natl. Acad. Sci. USA.* 91: 3127–3131.

48. Rousseau, F., J. W. Schymkowitz, and L. S. Itzhaki. 2003. The unfolding story of three-dimensional domain swapping. *Structure.* 11: 243–251.

49. Rousseau, F., J. Schymkowitz, and L. S. Itzhaki. 2012. Implications of 3D domain swapping for protein folding, misfolding and function. *Adv. Exp. Med. Biol.* 747:137–152.

50. Qu, C., L. Liljas, …, T. Lin. 2000. 3D domain swapping modulates the stability of members of an icosahedral virus group. *Structure.* 8:1095–1103.

51. Parker, M. J., C. E. Dempsey, …, A. R. Clarke. 1998. Topology, sequence evolution and folding dynamics of an immunoglobulin domain. *Nat. Struct. Biol.* 5:194–198.

52. Hayes, M. V., R. B. Sessions, …, A. R. Clarke. 1999. Engineered assembly of intertwined oligomers of an immunoglobulin chain. *J. Mol. Biol.* 285:1857–1867.

53. Schymkovitz, J. W., F. Rousseau, …, L. S. Itzhaki. 2000. The folding pathway of the cell-cycle regulatory protein p13 suc1: clues for the mechanism of domain swapping. *Structure.* 8:89–100.

54. Schymkowitz, J. W., F. Rousseau, …, L. S. Itzhaki. 2001. Observation of signal transduction in three-dimensional domain swapping. *Nat. Struct. Biol.* 8:888–892.

55. Rousseau, F., J. W. Schymkowitz, …, L. S. Itzhaki. 2001. Three-dimensional domain swapping in p13suc1 occurs in the unfolded state and is controlled by conserved proline residues. *Proc. Natl. Acad. Sci. USA.* 98:5596–5601.

56. Kirsten Frank, M., F. Dyda, …, A. M. Gronenborn. 2002. Core mutations switch monomeric protein GB1 into an intertwined tetramer. *Nat. Struct. Biol.* 9:877–885.

57. Rousseau, F., J. W. Schymkowitz, …, L. S. Itzhaki. 2004. Intermediates control domain swapping during folding of p13suc1. *J. Biol. Chem.* 279:8368–8377.

58. Liu, L., I. J. Byeon, …, A. M. Gronenborn. 2012. Domain swapping proceeds via complete unfolding: a ^{19}F- and ^{1}H-NMR study of the Cyanovirin-N protein. *J. Am. Chem. Soc.* 134:4229–4235.

59. Kang, X., N. Zhong, …, B. Xia. 2012. Foldon unfolding mediates the interconversion between M(pro)-C monomer and 3D domain-swapped dimer. *Proc. Natl. Acad. Sci. USA.* 109:14900–14905.

60. Yoo, S., D. G. Myszka, …, W. I. Sundquist. 1997. Molecular recognition in the HIV-1 capsid/cyclophilin A complex. *J. Mol. Biol.* 269: 780–795.

61. del Alamo, M., J. L. Neira, and M. G. Mateu. 2003. Thermodynamic dissection of a low affinity protein-protein interface involved in human immunodeficiency virus assembly. *J. Biol. Chem.* 278:27923–27929.

62. Sancho, J., and A. R. Fersht. 1992. Dissection of an enzyme by protein engineering. The N and C-terminal fragments of barnase form a native-like complex with restored enzymic activity. *J. Mol. Biol.* 224: 741–747.

63. Tinoco, I., K. Sauer, and J. C. Wang. 1995. Physical Chemistry, 3rd ed. Prentice Hall, Upper Saddle River, NJ.

64. Piotto, M., V. Saudek, and V. Sklenár. 1992. Gradient-tailored excitation for single-quantum NMR spectroscopy of aqueous solutions. *J. Biomol. NMR.* 2:661–665.

65. Myers, J. K., C. N. Pace, and J. M. Scholtz. 1995. Denaturant m values and heat capacity changes: relation to changes in accessible surface areas of protein unfolding. *Protein Sci.* 4:2138–2148.

66. Clish, C. B., D. H. Peyton, and E. Barklis. 1998. Solution structures of human immunodeficiency virus type 1 (HIV-1) and moloney murine leukemia virus (MoMLV) capsid protein major-homology-region peptide analogs by NMR spectroscopy. *Eur. J. Biochem.* 257:69–77.

67. Kingston, R. L., and V. M. Vogt. 2005. Domain swapping and retroviral assembly. *Mol. Cell.* 17:166–167.

68. Zhou, H.-X., G. Rivas, and A. P. Minton. 2008. Macromolecular crowding and confinement: biochemical, biophysical, and potential physiological consequences. *Annu Rev Biophys.* 37:375–397.

69. del Alamo, M., G. Rivas, and M. G. Mateu. 2005. Effect of macromolecular crowding agents on human immunodeficiency virus type 1 capsid protein assembly in vitro. *J. Virol.* 79:14271–14281.

70. Vriend, G. 1990. WHAT IF: a molecular modeling and drug design program. *J. Mol. Graph.* 8:52–56.

71. DeLano, W. L. 2002. Pymol molecular graphics system on World Wide Web. DeLano Scientific, San Carlos, CA. *http://www.pymol.org*.